

# CSC-Unet: A Novel Convolutional Sparse Coding Strategy based Neural Network for Semantic Segmentation

Haitong Tang, Shuang He, Xia Lu, Qin Yu, Kaiyue Liu, Hongjie Yan and Nizhuan Wang\*

**Abstract**—It is a challenging task to accurately perform semantic segmentation due to the complexity of real picture scenes. Many semantic segmentation methods based on traditional deep learning insufficiently captured the semantic and appearance information of images, which put limit on their generality and robustness for various application scenes. In this paper, we proposed a novel strategy that reformulated the popularly-used convolution operation to multi-layer convolutional sparse coding block to ease the aforementioned deficiency. This strategy can be possibly used to significantly improve the segmentation performance of any semantic segmentation model that involves convolutional operations. To prove the effectiveness of our idea, we chose the widely-used U-Net model for the demonstration purpose, and we designed CSC-Unet model series based on U-Net. Through extensive analysis and experiments, we provided credible evidence showing that the multi-layer convolutional sparse coding block enables semantic segmentation model to converge faster, can extract finer semantic and appearance information of images, and improve the ability to recover spatial detail information. The best CSC-Unet model significantly outperforms the results of the original U-Net on three public datasets with different scenarios, i.e., 87.14% vs. 84.71% on DeepCrack dataset, 68.91% vs. 67.09% on Nuclei dataset, and 53.68% vs. 48.82% on CamVid dataset, respectively.

**Index Terms**—U-Net, Semantic segmentation, Deep learning, Convolution operation, Convolutional sparse coding

## I. INTRODUCTION

In reality, the increasing application scenarios require inferring relevant knowledge or semantics from images; as a result, the importance of semantic segmentation for scene

This work was supported by National Natural Science Foundation of China (No. 41506106, 61701318, 82001160), Project of “Six Talent Peaks” of Jiangsu Province (No. SWYY-017), Project of Huaguoshan Mountain Talent Plan - Doctors for Innovation and Entrepreneurship, Jiangsu University Superior Discipline Construction Project Funding Project (PAPD), Jiangsu Province Graduate Research and Practice Innovation Program Project. (*Corresponding author: Nizhuan Wang*)

Haitong Tang, Shuang He, Xia Lu, Qin Yu, Kaiyue Liu, Nizhuan Wang are with School of Computer Engineering and School of Marine Technology and Geomatics, Jiangsu Key Laboratory of Marine Bioresources and Environment, Jiangsu Key Laboratory of Marine Biotechnology, Jiangsu Ocean University, Lianyungang, 222023, China (e-mails: httang1224@gmail.com; kyrohe95@gmail.com; lux2008000070@jou.edu.cn; vpz.sch@gmail.com; liukaiyue66998@gmail.com; wangnizhuan1120@gmail.com).

Hongjie Yan is with Department of Neurology, Affiliated Lianyungang Hospital of Xuzhou Medical University, Lianyungang 222002, China (e-mail: yanhjns@gmail.com)

understanding is gradually increasing. Semantic segmentation gives us more detailed understanding of images than image classification [1]–[5] or object detection [6]–[13]. This understanding is crucial in many different domains such as autonomous driving, robotics, image search engines, etc.

Recently, a lot of semantic segmentation methods have emerged. For example, fully convolutional networks (FCN) [14], at an end to end form, has firstly implemented semantic segmentation on pixel-wise prediction task, achieving relatively better results in natural scene image segmentation. SegNet [15] makes the model more efficient than FCN by introducing more skip architecture and max-pooling indexes. PSPNet [16] used dilated convolution and pyramid pooling to improve SegNet. U-Net [17] was proposed in the 2015 ISBI competition, which consists of contracting and symmetrically expanding sub-networks to form a U-shaped architecture. This model was originally designed to solve biomedical image segmentation. Since it requires a small number of training samples to achieve good segmentation results, it is widely used in various directions of semantic segmentation. Other excellent semantic segmentation models include DeepLab series [18]–[21], SFNet[22], etc.[23]–[27].

All the above semantic segmentation models are based on convolution operations, which have strong feature representation capabilities to extract semantic (global) and appearance (local) information of images. However, for the segmentation task of complex image, it is usually limited by the semantic and appearance information extracted from the shallow convolution layers. As a rule, they mostly choose to deepen the network layers so that the semantic segmentation network can better capture the semantic and appearance information of the images to improving the segmentation performance. However, if the network keeps deepening indefinitely, there is a tremendous challenge for both the computational power and the optimizer. Thus, we should solve this problem at the root by optimizing the convolution operation.

In this paper, we proposed a novel strategy in semantic segmentation model which reformulated convolution operation to multi-layer convolutional sparse coding (ML-CSC) block. Taking the U-Net as an example, we demonstrated the effectiveness and robustness of ML-CSC block strategy in the designed CSC-Unet model series, and it can also be potentially applied to other excellent semantic segmentation networks,

such as SegNet, DeepLab series, etc. Benefit from the advantages of ML-CSC block in information representation compared to convolutional operation. We hypothesize that the CSC-Unet model series has the superiorities of better captured semantic and appearance information of original images, better spatial detail information, and better convergence efficiency without increasing the trainable parameters. We will validate these merits in the subsequent experiments.

As far as we are aware, it is the first work to explore semantic segmentation based on convolutional sparse coding. We hope that our strategy can provide ideas for subsequently designing excellent semantic segmentation models. There contributions are summarized as follows:

1) We propose a novel strategy to use the multi-layer convolutional sparse coding blocks instead of convolution operation in semantic segmentation networks.

2) We apply ML-CSC block to U-Net semantic segmentation model, and through extensive experiments we demonstrate the advantages and feasibility of this strategy.

3) We further explore the impact of the number of unfoldings in the ML-CSC block on the performance of the semantic segmentation model.

4) Our strategy can enhance the structure of semantic segmentation model and can extend the idea of semantic segmentation model based on traditional convolution operation.

The rest of this paper is summarized as follows. Section II will give a brief introduction of the theory of multi-layer convolutional sparse coding and ML-CSC block. In Section III, we will present the design details of CSC-Unet model series. The procedure and results of the experiments are presented in Section IV. Section V is the conclusion and future work that we will carry out.

## II. BRIEF INTRODUCTION OF MULTI-LAYER CONVOLUTIONAL SPARSE CODING

In this section, we firstly reviewed the multi-layer convolutional sparse coding model and its solution algorithm, then we presented the details of the designed ML-CSC block.

### A. Multi-Layer Convolutional Sparse Coding Model

The ML-CSC model [28] assumes that the input image  $y$  satisfies multi-layer convolutional sparse coding model, it can be denoted as:

$$\begin{aligned} y &= D_1 \Gamma_1, \\ \Gamma_1 &= D_2 \Gamma_2, \\ &\vdots \\ \Gamma_{L-1} &= D_L \Gamma_L. \end{aligned} \quad (1)$$

where  $\{D_i\}_{i=1}^L$  are special dictionaries, each  $D_i$  is a transpose of a convolutional matrix  $W_i$ .

$$D_i = W_i^T \quad (2)$$

### B. The Solver of Multi-Layer Convolutional Sparse Coding Model

1) *Layered Thresholding Algorithm*: Finding  $\{\Gamma_i\}_{i=1}^L$  at once is NP-hard and challenging in computation and concept. Papyan et al. [28] proposed the layered thresholding algorithm, that computes the sparse vectors  $\{\Gamma_i\}_{i=1}^L$  step by step in different layers. The solve can be written that:

$$\begin{aligned} \hat{\Gamma}_1 &= h_{\theta_1} (D_1^T y) = \text{ReLU}(\mu_1 D_1^T y + \theta_1), \\ \hat{\Gamma}_2 &= h_{\theta_2} (D_2^T \hat{\Gamma}_1) = \text{ReLU}(\mu_2 D_2^T \hat{\Gamma}_1 + \theta_2), \\ &\vdots \\ \hat{\Gamma}_L &= h_{\theta_L} (D_L^T \hat{\Gamma}_{L-1}) = \text{ReLU}(\mu_L D_L^T \hat{\Gamma}_{L-1} + \theta_L). \end{aligned} \quad (3)$$

where  $\{\mu_i\}_{i=1}^L$  and  $\{\theta_i\}_{i=1}^L$  are trainable parameters. Combined with Equation 2, the above equation can be written as:

$$\begin{aligned} \hat{\Gamma}_1 &= \text{ReLU}(\mu_1 W_1 y + \theta_1), \\ \hat{\Gamma}_2 &= \text{ReLU}(\mu_2 W_2 \hat{\Gamma}_1 + \theta_2), \\ &\vdots \\ \hat{\Gamma}_L &= \text{ReLU}(\mu_L W_L \hat{\Gamma}_{L-1} + \theta_L). \end{aligned} \quad (4)$$

2) *Layered Iterative Soft Thresholding Algorithm*: It is well known that thresholding algorithm is the simplest and dumbest pursuit algorithm for sparse signals. Papyan et al. [29] proposed a more complex and accurate alternative layered pursuit algorithm based on the Basis Pursuit algorithm [30]. Accordingly, our goal is to solve the following equations:

$$\begin{aligned} \hat{\Gamma}_1 &= \arg \min_{\Gamma_1} \frac{1}{2} \|\hat{\Gamma}_0 - D_1 \Gamma_1\|_2^2 + \lambda_1 \|\Gamma_1\|_1, \\ \hat{\Gamma}_2 &= \arg \min_{\Gamma_2} \frac{1}{2} \|\hat{\Gamma}_1 - D_2 \Gamma_2\|_2^2 + \lambda_2 \|\Gamma_2\|_1, \\ &\vdots \\ \hat{\Gamma}_L &= \arg \min_{\Gamma_L} \frac{1}{2} \|\hat{\Gamma}_{L-1} - D_L \Gamma_L\|_2^2 + \lambda_L \|\Gamma_L\|_1. \end{aligned} \quad (5)$$

where  $\hat{\Gamma}_0 = y$ , and  $\|\cdot\|_1$  is sparsity regularization constraint term [31].  $\{\lambda_i\}_{i=1}^L$  are regularization parameters to control the sparsity of  $\{\Gamma_i\}_{i=1}^L$ . An attractive approximate solver of the layered-BP algorithm is the multi-layer iterative soft thresholding algorithm [32], which can be derived that:

$$\begin{aligned} \hat{\Gamma}_1 &= \hat{\Gamma}_1^k = \text{ReLU}\left(\tilde{\Gamma}_1 - \mu_1 D_1^T \left(D_1 \tilde{\Gamma}_1 - \hat{\Gamma}_0^k\right) + \theta_1\right), \\ \hat{\Gamma}_2 &= \hat{\Gamma}_2^k = \text{ReLU}\left(\tilde{\Gamma}_2 - \mu_2 D_2^T \left(D_2 \tilde{\Gamma}_2 - \hat{\Gamma}_1^k\right) + \theta_2\right), \\ &\vdots \\ \hat{\Gamma}_L &= \hat{\Gamma}_L^k = \text{ReLU}\left(\tilde{\Gamma}_L - \mu_L D_L^T \left(D_L \tilde{\Gamma}_L - \hat{\Gamma}_{L-1}^k\right) + \theta_L\right). \end{aligned} \quad (6)$$

Combined with Equation 2, the above equation can be written as:

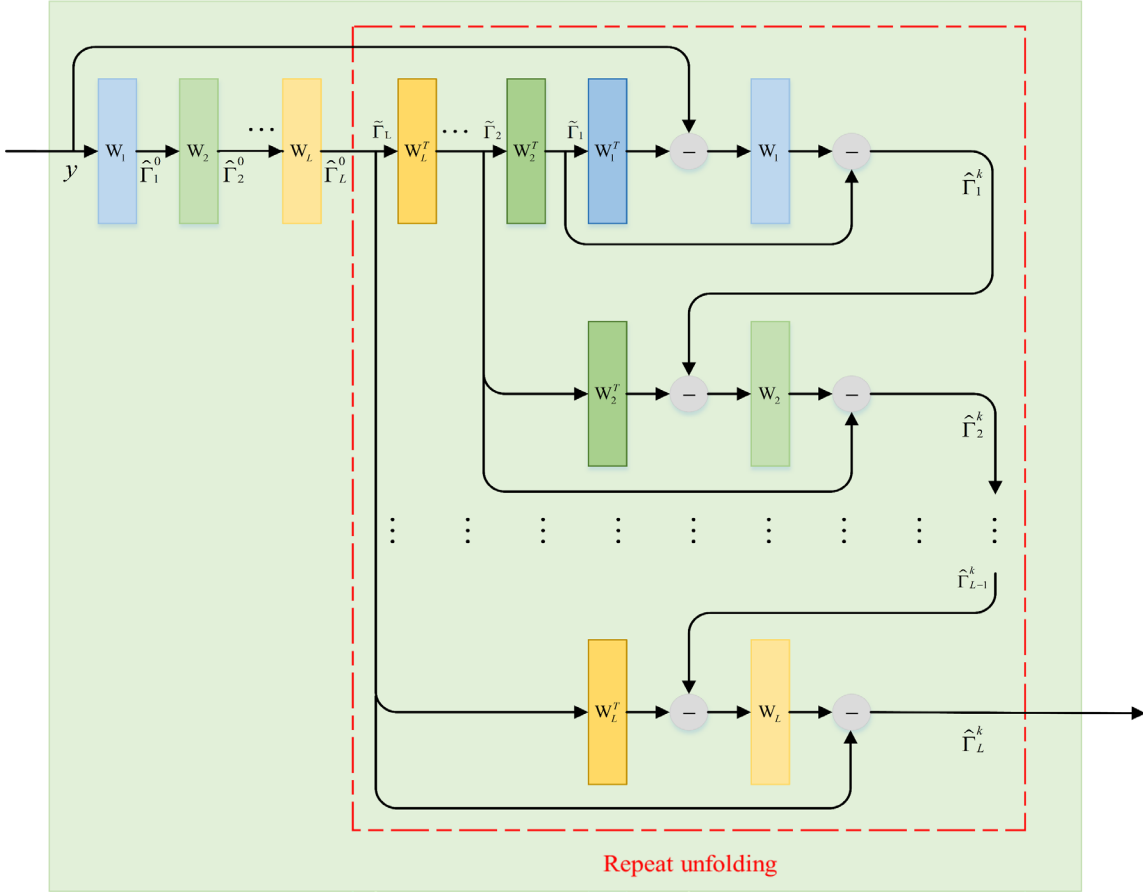


Fig. 1. The ML-CSC block.  $\{W_i\}_{i=1}^L$  denote the convolution operation,  $\{W_i^T\}_{i=1}^L$  denote the deconvolution operation,  $L$  denotes the number of layers, and  $k$  denotes unfolding number.

$$\begin{aligned}
 \hat{\Gamma}_1 &= \text{ReLU}\left(\tilde{\Gamma}_1 - \mu_1 W_1 \left(W_1^T \tilde{\Gamma}_1 - \hat{\Gamma}_0^k\right) + \theta_1\right), \\
 \hat{\Gamma}_2 &= \text{ReLU}\left(\tilde{\Gamma}_2 - \mu_2 W_2 \left(W_2^T \tilde{\Gamma}_2 - \hat{\Gamma}_1^k\right) + \theta_2\right), \\
 &\vdots \\
 \hat{\Gamma}_L &= \text{ReLU}\left(\tilde{\Gamma}_L - \mu_L W_L \left(W_L^T \tilde{\Gamma}_L - \hat{\Gamma}_{L-1}^k\right) + \theta_L\right).
 \end{aligned} \tag{7}$$

### C. Multi-Layer Convolutional Sparse Coding Block

In the multi-layer convolutional sparse coding model, we summarize the solving process as shown in Fig. 1, and name it as ML-CSC block.  $\{W_i\}_{i=1}^L$  denotes the convolution operation.

$\{W_i^T\}_{i=1}^L$  denotes the deconvolution operation.  $\{\mu_i\}_{i=1}^L$  and  $\{\theta_i\}_{i=1}^L$  are trainable parameters. The ML-CSC block performs the layered thresholding algorithm when the number of unfoldings is 0. Solving  $\Gamma_L$  can be seen as the process of extracting features from multi-layer convolution operation.

$$\Gamma_L = \text{ReLU}\left(W_L \cdots \text{ReLU}\left(W_2 \text{ReLU}\left(W_1 y\right)\right)\right) \tag{8}$$

In that we ignore the trainable parameters for simplicity of presentation. When the unfolding number is greater than 0, the multi-layer iterative soft thresholding algorithm (ML-ISTA) is

executed. If there is no special case, in this paper we default the number of unfoldings of ML-CSC block is greater than 0. From the sparse point of view, due to multi-layer iterative soft thresholding algorithm is superior to the layered thresholding algorithm, the ML-CSC block will extract more accurate  $\hat{\Gamma}_L$  compared with multi-layer convolution operation, which is beneficial for the forward propagation of the neural network and also can better capture the semantic and appearance information of the image to improve the segmentation performance.

## III. METHOD

To demonstrate our strategy on the U-Net model, we designed a series of CSC-Unet models, and this section will show the design ideas and details of these models. The implementation of CSC-Unet models is available at <https://github.com/NZWANG/CSC-Unet>.

### A. U-Net Model

There are some minor differences between the U-Net we used and the one in [17]. For convenience, we use  $3 \times 3$  convolution layer with padding to keep the same size before and after convolution operation, thus the input size of model is

TABLE I  
THE DETAILS OF MODELS

Model	U-Net	CSC-Unet-Encode	CSC-Unet-Decode	CSC-Unet-All
Encode	$[2 \times \text{Conv2d}] \times 5$	$[\text{ML-CSC block}] \times 5$	$[2 \times \text{Conv2d}] \times 5$	$[\text{ML-CSC block}] \times 5$
Decode	$[2 \times \text{Conv2d}] \times 4$	$[2 \times \text{Conv2d}] \times 4$	$[\text{ML-CSC block}] \times 4$	$[\text{ML-CSC block}] \times 4$

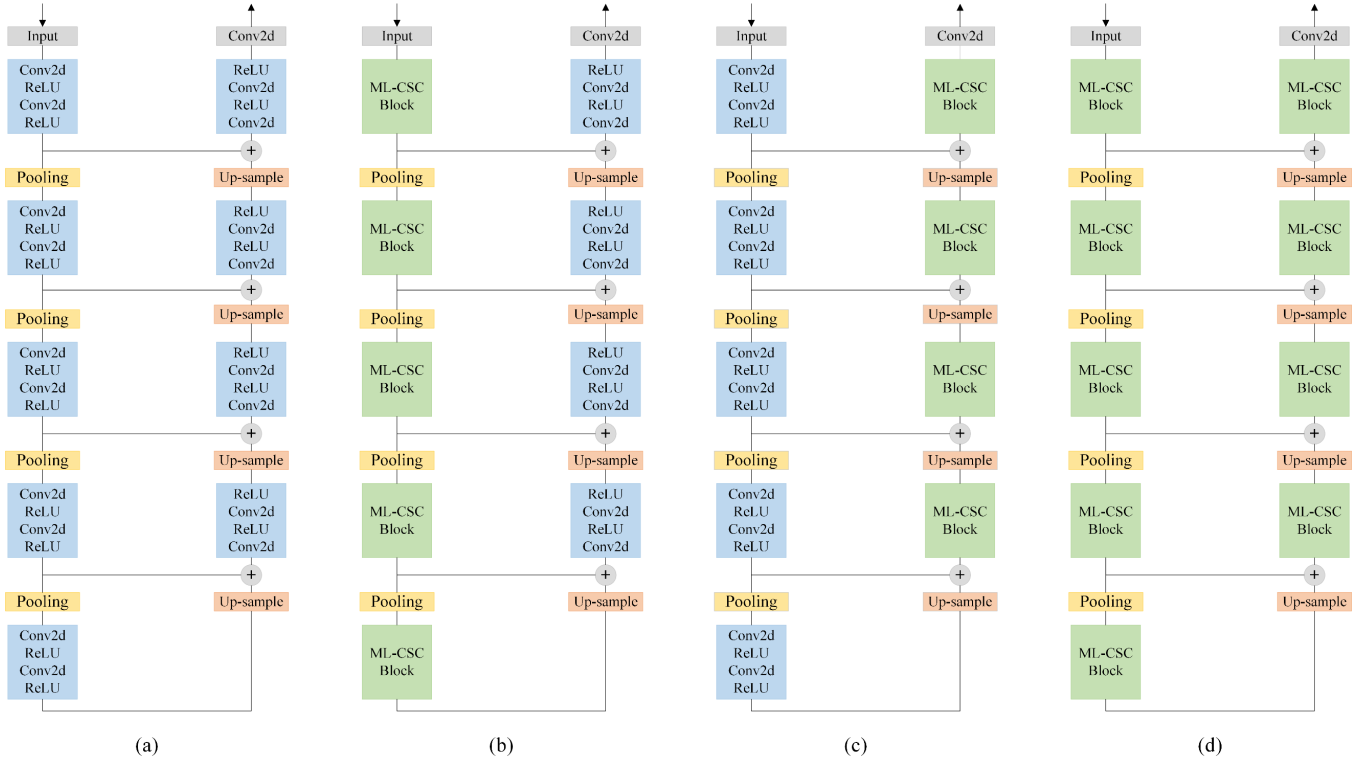


Fig. 2. Structures of (a) U-Net, (b) our CSC-Unet-Encode, (c) our CSC-Unet-Decode, and (d) our CSC-Unet-All, respectively.

equal to the output size. The up-sampling is performed by  $3 \times 3$  transposed convolution operation. Batch normalization (BN) [33] is after convolution operation and before rectified linear unit (ReLU) activation function [34]. The U-Net model is displayed in Fig. 2(a).

### B. CSC-Unet Model Series

In the encode and decode side of the U-Net model, both of which can be seen as a composition of blocks containing two layers of convolution operation, as shown in Table I. To fairly demonstrate our strategy, we set the number of layers in the ML-CSC block to 2 as well. According to the characteristics of U-Net encoding and decoding structure, we designed a host of CSC-Unet-model series including CSC-Unet-Encode, CSC-Unet-Decode, and CSC-Unet-All model. The details of the CSC-Unet model series were also shown in Table I.

1) *CSC-Unet-Encode Model*: The encoding side of U-Net is used to extract the semantic and appearance information of the input picture. In order to explore the ability of ML-CSC block to extract information in semantic segmentation, we replaced the convolution operations of the encoding side of the U-Net with the ML-CSC blocks to form CSC-Unet-Encode model, as shown in Fig. 2(b).

2) *CSC-Unet-Decode Model*: In the expanding sub-network of U-Net model, it firstly uses skip connection to combine

appearance information from the shallow layers and semantic information from the deep layers. Then, the decoding side of U-Net precisely locates the segmentation boundary and gradually recovers the spatial detail information of the image. To explore the ability of ML-CSC block to recover the spatial detail information of image, we introduced the ML-CSC block into the decoding side of U-Net to form CSC-Unet-Encode model, as shown in Fig. 2(c).

3) *CSC-Unet-All Model*: To explore the impact of ML-CSC block on the overall segmentation performance of U-Net model, we added this block to both the encoding and decoding side of the U-Net to form CSC-Unet-All model, as shown in Fig. 2(d).

## IV. EXPERIMENT AND ANALYSIS

In this research, the computing devices are Ubuntu 18.04.5 LTS 64-bit OS, 32G RAM, and Nvidia GeForce GTX 1080 Ti GPU with 11 GB memory. The deep learning framework is based on PyTorch [35].

### A. Datasets

For perform a fair evaluation, we select different scenarios datasets for testing to obtain evaluation metrics of comparison models. CamVid [36] is one of the first datasets used for

TABLE II  
THE DETAILS OF DATASETS USED IN THE EXPERIMENT

Dataset	Classes	Samples (training)	Samples (validation)	Samples (test)	Samples (total)
CamVid	11	367	101	233	701
DeepCrack	2	322	107	108	537
Nuclei	3	402	134	134	670

TABLE III  
RESULT ON DEEPCRACK, NUCLEI AND CAMVID TEST SET OF CSC-UNET-ENCODE MODELS

Method	DeepCrack Mean IoU (%)	Nuclei Mean IoU (%)	CamVid Mean IoU (%)
U-Net (CSC-Unet-Encode-0)	84.71	67.09	48.82
CSC-Unet-Encode-1	86.41	67.26	52.31
CSC-Unet-Encode-2	<b>86.90</b>	<b>68.44</b>	<b>53.29</b>
CSC-Unet-Encode-3	86.20	67.71	52.43

autonomous driving. It is assembled from 5 video sequences taken by the on-board camera from the driver's perspective. DeepCrack [37] is a public benchmark dataset containing cracks at multiple scales and scenarios to evaluate crack detection systems. Nuclei<sup>1</sup> is the dataset in the 2018 Kaggle Data Science Bowl which was acquired under a variety of conditions and variations in the cell type, magnification, and imaging modality. The details of the datasets were shown in Table II.

### B. The setting of Training Parameters

The number of all epochs were empirically set to 200 in this experiment. To improve the generalization ability of the model, before each epoch, we randomly disrupted the training data to make it more consistent with the sample distribution under natural conditions. The batch size was set to 4. The loss function was negative log-likelihood, and the input parameters were activated by the log-SoftMax function. The model used Adam [38] algorithm as the optimizer, each 50 epochs, and the learning rate dropped by half. In the CamVid. The initial learning rate was set to  $10^{-4}$ , for the DeepCrack and Nuclei, the initial learning rate was set to  $10^{-5}$ , respectively.

### C. Experiment and Analysis

1) *The Speed of Model Convergence:* We investigated the effect of ML-CSC blocks on the convergence speed of segmentation models. On the DeepCrack dataset, we compared the training and validation loss of the models with the different number of blocks in the training phase, and the results were shown in Fig. 3. We found that ML-CSC blocks can accelerate the convergence of the semantic segmentation model and reduce the loss value. Adding ML-CSC blocks at the decoding side of the U-Net model converged faster than adding them at the encoding side, and the model converged fastest when ML-CSC blocks were added at both sides of U-Net.

2) *The Extraction of Semantic and Appearance Information:* We have assessed the influence of ML-CSC block on CSC-Unet model series compared with U-Net to extract semantic and appearance information, and the results were shown in Table III, where the number after the model indicated

the unfolding number of ML-CSC block. When the number of unfoldings was 0, the CSC-Unet-Encode was equivalent to the U-Net model. The results showed that CSC-Unet-Encode models outperformed U-Net model on all three datasets when the number of unfoldings was greater than 0. This indicated that the ML-CSC block can indeed improve the ability of the semantic segmentation model to capture the semantic and appearance information of the image. Furthermore, we found that it was not always true that the larger number of unfoldings of the ML-CSC block implied better performance.

Semantic segmentation model first extracts feature information at the encoding side, and then based on feature information the model gradually recovers the spatial detail information of the image at the decoding side. As the number of unfoldings increases, the feature information conveys in the model becomes sparser, which is not beneficial for the recovery process at the decoding side. Therefore, we should find a balance point between the extraction of feature information and the recovery process. According to Table III, we inferred that the balance point was reached when the unfolding number was 2 among most datasets. For the convenience of performance

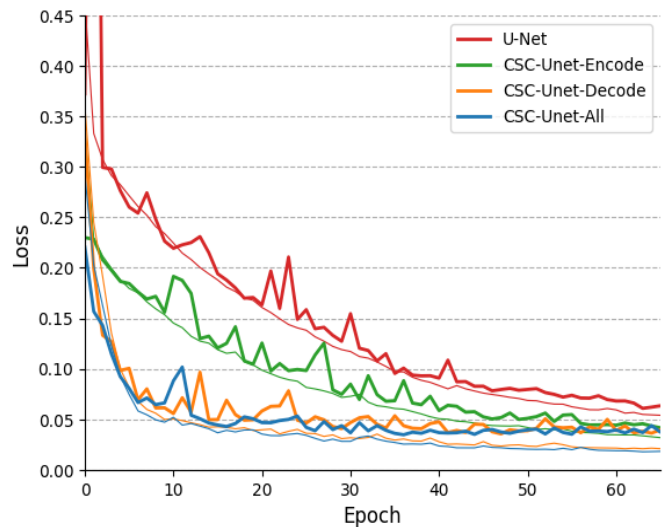


Fig. 3. Training on DeepCrack. Fine curves indicate the loss of training, and thick curves indicate the loss of validation. Unfolding number is uniformly set to 2 and the trainable parameters are same for all models.

<sup>1</sup> <https://www.kaggle.com/c/data-science-bowl-2018/overview>

TABLE IV  
RESULT ON DEEPCRACK, NUCLEI AND CAMVID TEST SET OF CSC-UNET-DECODE MODELS

Method	DeepCrack Mean IoU (%)	Nuclei Mean IoU (%)	CamVid Mean IoU (%)
U-Net (CSC-Unet-Decode-0)	84.71	67.09	48.42
CSC-Unet-Decode-1	<b>86.29</b>	<b>68.20</b>	51.49
CSC-Unet-Decode-2	85.52	67.24	52.33
CSC-Unet-Decode-3	85.21	67.25	<b>53.18</b>

TABLE V  
RESULT ON DEEPCRACK AND NUCLEI TEST SET OF THE CSC-UNET-ALL MODELS

Method	DeepCrack		Nuclei	
	Pixel Acc (%)	Mean IoU (%)	Pixel Acc (%)	Mean IoU (%)
U-Net (CSC-Unet-All-0-0)	98.53	84.71	96.64	67.09
CSC-Unet-All-2-1 (best)	<b>98.74</b>	<b>87.14</b>	<b>96.81</b>	<b>68.91</b>
CSC-Unet-All-1-1	98.62	86.61	96.67	67.30
CSC-Unet-All-2-2	98.72	87.04	96.73	68.31

TABLE VI  
RESULTS ON CAMVID TEST SET OF CSC-UNET-ALL MODELS (1) U-NET(CSC-UNET-ALL-0-0), (2) CSC-UNET-ALL-2-1, (3) CSC-UNET-ALL-1-1 AND (4) CSC-UNET-ALL-2-2

Model	Sky	Building	Pole	Road	Sidewalk	Tree	Sign	Fence	Car	Pedestrian	Building	Class avg. (%)	Mean IOU (%)
(1)	<b>96.6</b>	75.9	27.7	96.4	75.1	81.2	<b>50.1</b>	16.3	<b>87.0</b>	43.6	10.9	60.1	48.82
(2)	96.1	84.6	33.4	97.6	85.2	81.2	45.6	<b>18.4</b>	86.0	54.8	12.5	63.2	53.56
(3)	95.9	80.5	33.6	<b>97.8</b>	<b>85.8</b>	82.8	41.8	15.2	85.5	<b>60.6</b>	<b>14.5</b>	63.1	52.76
(4)	95.5	<b>87.5</b>	<b>36.6</b>	97.6	83.3	<b>82.9</b>	38.4	16.5	86.0	59.6	12.2	<b>63.3</b>	<b>53.68</b>

demonstration, in our all experiments, the maximum number of unfoldings was set to 3.

3) *The Ability to Recover Spatial Detail Information:* Next, we explored the ability of ML-CSC block to recover spatial detail information of image at the decoding side and the results were shown in Table IV. CSC-Unet-Decode models with unfolding number greater than 0 on different datasets were better than U-Net, which implied that ML-CSC block improved the recovery of spatial detail information compared to the convolution operation. The best unfolding was 1 in DeepCrack and Nuclei, and in CamVid was 3, respectively. We speculated that was probably related to the complexity of the image, where the categories of DeepCrack and Nuclei were relatively few and the case of 1 unfoldings was enough, but CamVid was relatively more complex and required a higher number of unfoldings.

4) *The Overall Improvement of Model Performance:* We first introduced the nomenclature of CSC-Unet-All-a-b, where a denoted the unfolding number at the encoding side and b denoted the number of unfoldings at the decoding side. For example, CSC-Unet-All-0-0 was equivalent to U-Net model, CSC-Unet-All-a-0 was represented as CSC-Unet-Encode-a, and CSC-Unet-All-0-b can be represented as CSC-Unet-Decode-b. Through Table III and IV, we found that on the DeepCrack dataset the CSC-Unet-Encode-1 captured more semantic and appearance information, and CSC-Unet-Decode-2 maximized the ability of the model to recover spatially detailed information. Thus, we argued that CSC-Unet-All-2-1 can maximize the segmentation performance of the U-Net model. Similarly, on Nuclei and

CamVid, CSC-Unet-All-2-1 and CSC-Unet-All-2-3 should achieve the best segmentation performance. However, due to the GPU memory size limitation, if we use the CSC-Unet-All-2-3 model on the CamVid dataset, the batch size needs to be halved, or we can use GPU parallelism to maintain the batch size. This is something that we do not expect to see. We want to compare the performance of the models under the same conditions; thus, we used CSC-Unet-All-2-2 instead of CSC-Unet-All-2-3. We also set CSC-Unet-All-0-0 (U-Net) and CSC-Unet-All-1-1 for performance comparison. The results on the three datasets were shown in Table V and VI. Compared to U-Net we have improved by 2.43% (from 84.71% to 87.14% in DeepCrack), 1.82% (from 67.09% to 68.91% in Nuclei), and 4.86% (from 48.82% to 53.68% in CamVid) on three datasets in terms of Mean Intersection over Union (MIoU), respectively. To better illustrate the results, the visualizations on the three datasets were shown in Fig. 4.

## V. CONCLUSION AND DISCUSSION

In this paper, we proposed a novel strategy which used multi-layer convolutional sparse coding block instead of convolutional operation to improve the performance of semantic segmentation model. This strategy can be possibly applied to any semantic segmentation model that involved convolutional operation. We used the U-Net model as an example to validate this strategy and designed CSC-Unet model series. We found that using ML-CSC blocks instead of convolution operations can accelerate the convergence of the semantic segmentation model, improve the ability of the model

to capture the semantic and appearance information of the image, and improve the ability to recover spatial detail

information. We concluded that ML-CSC block was a better

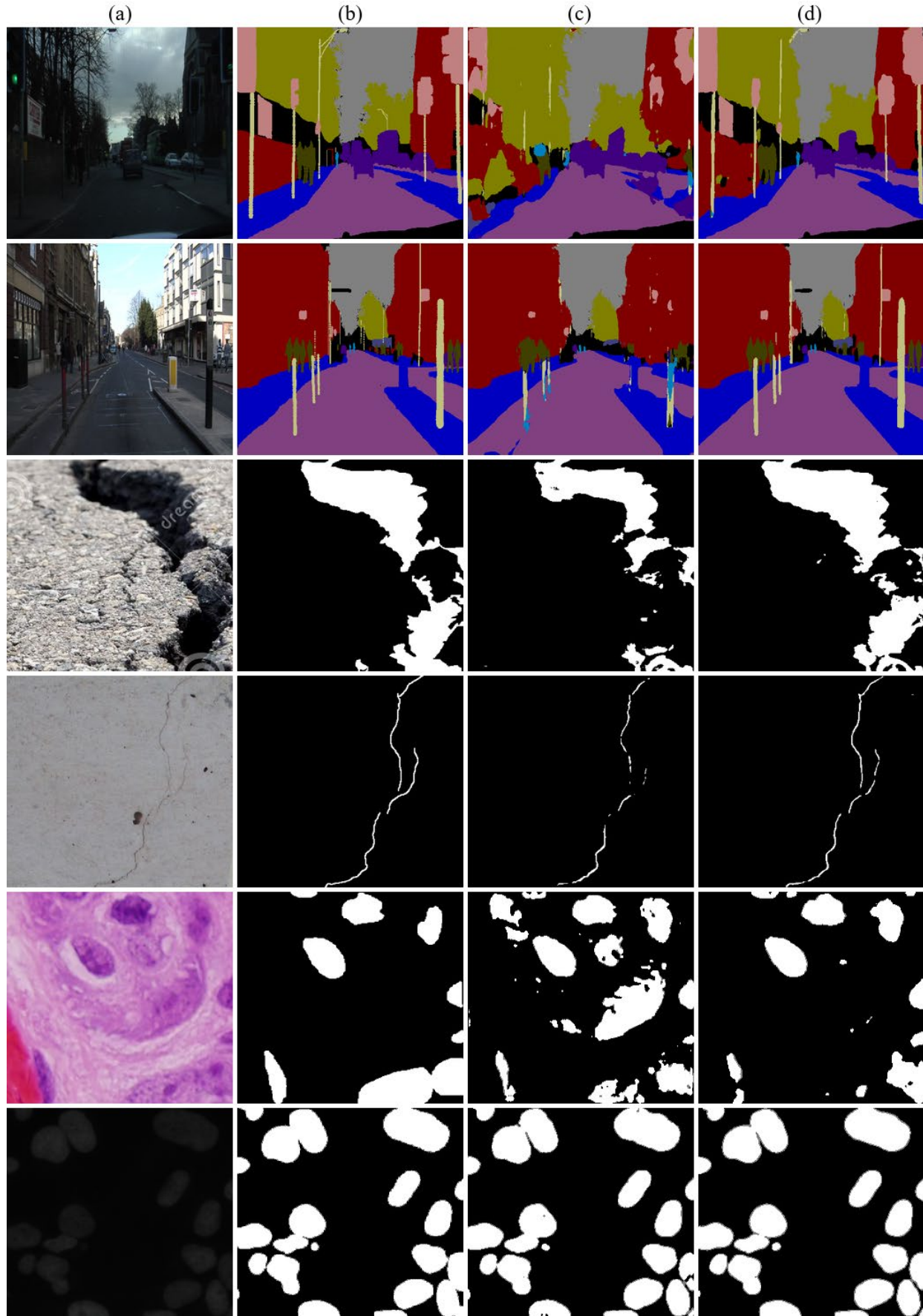


Fig. 4. Examples of semantic segmentation results on CamVid, DeepCrack, and Nuclei test set. (a) Input images, (b) Ground truths, (c) Results of U-Net, and (d) Results of CSC-Unet-All (best).

operation compared to convolutional operation in semantic segmentation.

The current CSC-Unet models have achieved significant improvement in segmentation performance compared with the original U-Net model. However, they still face great challenges. Therefore, in the follow-up study, we will consider the following aspects.

1) To fairly demonstrate our strategy, the added ML-CSC block to the U-Net model was a two-layer convolutional sparse coding model. We believe that two layers are still too short, which might limit the performance of semantic segmentation. In the next study, we will design a new type of semantic segmentation model based on multi-layer global convolutional sparse coding block.

2) In order that our proposed strategy was not influenced by other operations, we just added the ML-CSC block in this research. We do not use any pre-processing, post-processing operations, and other operations that can significantly improve accuracy. But in subsequent studies, we will add these operations to maximize the performance of CSC-Unet models.

3) We found that there is a balance between the extraction of feature information and the recovery process. How to adaptively find the best balance among all the unfoldings will be one focus of our future research.

4) The ML-CSC block can be extended to not only the field of semantic segmentation, but also possibly to other fields such as object detection, generative adversarial networks (GAN) [39], and natural language processing (NLP) [40] in our subsequent research.

#### REFERENCES

- [1] A. Krizhevsky, I. Sutskever, and G. E. Hinton, "Imagenet classification with deep convolutional neural networks," *Adv. Neural Inf. Process. Syst.*, vol. 25, pp. 1097–1105, 2012.
- [2] K. Simonyan and A. Zisserman, "Very deep convolutional networks for large-scale image recognition," *arXiv Prepr. arXiv1409.1556*, 2014.
- [3] K. He, X. Zhang, S. Ren, and J. Sun, "Deep residual learning for image recognition," in *Proceedings of the IEEE Computer Society Conference on Computer Vision and Pattern Recognition*, 2016, vol. 2016-Decem, pp. 770–778, doi: 10.1109/CVPR.2016.90.
- [4] C. Szegedy *et al.*, "Going deeper with convolutions," *Proc. IEEE Comput. Soc. Conf. Comput. Vis. Pattern Recognit.*, vol. 07-12-June, pp. 1–9, 2015, doi: 10.1109/CVPR.2015.7298594.
- [5] H. Tang *et al.*, "Comparison of Convolutional Sparse Coding Network and Convolutional Neural Network for Pavement Crack Classification: A Validation Study," *J. Phys. Conf. Ser.*, vol. 1682, no. 1, p. 12016, 2020, doi: 10.1088/1742-6596/1682/1/012016.
- [6] S. Ren, K. He, R. Girshick, and J. Sun, "Faster r-cnn: Towards real-time object detection with region proposal networks," *arXiv Prepr. arXiv1506.01497*, 2015.
- [7] R. Girshick, J. Donahue, T. Darrell, and J. Malik, "Rich feature hierarchies for accurate object detection and semantic segmentation," in *Proceedings of the IEEE conference on computer vision and pattern recognition*, 2014, pp. 580–587.
- [8] J. Redmon and A. Farhadi, "Yolov3: An incremental improvement," *arXiv Prepr. arXiv1804.02767*, 2018.
- [9] W. Liu *et al.*, "Ssd: Single shot multibox detector," in *European conference on computer vision*, 2016, pp. 21–37.
- [10] R. Girshick, "Fast r-cnn," in *Proceedings of the IEEE international conference on computer vision*, 2015, pp. 1440–1448.
- [11] J. Redmon, S. Divvala, R. Girshick, and A. Farhadi, "You only look once: Unified, real-time object detection," *Proc. IEEE Comput. Soc. Conf. Comput. Vis. Pattern Recognit.*, vol. 2016-Decem, pp. 779–788, 2016, doi: 10.1109/CVPR.2016.91.
- [12] J. Redmon and A. Farhadi, "YOLO9000: Better, faster, stronger," *Proc. - 30th IEEE Conf. Comput. Vis. Pattern Recognition, CVPR 2017*, vol. 2017-Janua, pp. 6517–6525, 2017, doi: 10.1109/CVPR.2017.690.
- [13] A. Bochkovskiy, C. Y. Wang, and H. Y. M. Liao, "YOLOv4: Optimal Speed and Accuracy of Object Detection," *arXiv*, 2020.
- [14] J. Long, E. Shelhamer, and T. Darrell, "Fully convolutional networks for semantic segmentation," in *Proceedings of the IEEE conference on computer vision and pattern recognition*, 2015, pp. 3431–3440.
- [15] V. Badrinarayanan, A. Kendall, and R. Cipolla, "SegNet: A Deep Convolutional Encoder-Decoder Architecture for Image Segmentation," *IEEE Trans. Pattern Anal. Mach. Intell.*, vol. 39, no. 12, pp. 2481–2495, 2017, doi: 10.1109/TPAMI.2016.2644615.
- [16] H. Zhao, J. Shi, X. Qi, X. Wang, and J. Jia, "Pyramid scene parsing network," in *Proceedings of the IEEE conference on computer vision and pattern recognition*, 2017, pp. 2881–2890.
- [17] O. Ronneberger, P. Fischer, and T. Brox, "U-net: Convolutional networks for biomedical image segmentation," *Lect. Notes Comput. Sci. (including Subser. Lect. Notes Artif. Intell. Lect. Notes Bioinformatics)*, vol. 9351, pp. 234–241, 2015, doi: 10.1007/978-3-319-24574-4\_28.
- [18] L.-C. Chen, G. Papandreou, I. Kokkinos, K. Murphy, and A. L. Yuille, "Semantic image segmentation with deep convolutional nets and fully connected crfs," *arXiv Prepr. arXiv1412.7062*, 2014.
- [19] L.-C. Chen, G. Papandreou, I. Kokkinos, K. Murphy, and A. L. Yuille, "DeepLab: Semantic image segmentation with deep convolutional nets, atrous convolution, and fully connected crfs," *IEEE Trans. Pattern Anal. Mach. Intell.*, vol. 40, no. 4, pp. 834–848, 2017.
- [20] L. C. Chen, G. Papandreou, F. Schroff, and H. Adam, "Rethinking atrous convolution for semantic image segmentation," *arXiv*, 2017.
- [21] L. C. Chen, Y. Zhu, G. Papandreou, F. Schroff, and H. Adam, "Encoder-decoder with atrous separable convolution for semantic image segmentation," *arXiv*, 2018.
- [22] J. Lee, D. Kim, J. Ponce, and B. Ham, "SFNet: Learning object-aware semantic correspondence," *arXiv*, pp. 2278–2287, 2019.
- [23] C. Yu, J. Wang, C. Peng, C. Gao, G. Yu, and N. Sang, "BiSeNet: Bilateral segmentation network for real-time semantic segmentation," *Lect. Notes Comput. Sci. (including Subser. Lect. Notes Artif. Intell. Lect. Notes Bioinformatics)*, vol. 11217 LNCS, pp. 334–349, 2018, doi: 10.1007/978-3-030-01261-8\_20.
- [24] C. Li, W. Xia, Y. Yan, B. Luo, and J. Tang, "Segmenting objects in day and night: Edge-conditioned cnn for thermal image semantic segmentation," *IEEE Trans. Neural Networks Learn. Syst.*, 2020.
- [25] Z. Zhang, X. Zhang, C. Peng, X. Xue, and J. Sun, "ExFuse: Enhancing feature fusion for semantic segmentation," *Lect. Notes Comput. Sci. (including Subser. Lect. Notes Artif. Intell. Lect. Notes Bioinformatics)*, vol. 11214 LNCS, pp. 273–288, 2018, doi: 10.1007/978-3-030-01249-6\_17.
- [26] H. Noh, S. Hong, and B. Han, "Learning deconvolution network for semantic segmentation," *Proc. IEEE Int. Conf. Comput. Vis.*, vol. 2015 Inter, pp. 1520–1528, 2015, doi: 10.1109/ICCV.2015.178.
- [27] A. Zhu, Y. Zhu, N. Wang, and Y. Chen, "A robust self-driven surface crack detection algorithm using local features," *Insight Non-Destructive Test. Cond. Monit.*, vol. 62, no. 5, pp. 269–276, 2020, doi: 10.1784/insi.2020.62.5.269.
- [28] V. Papyan, Y. Romano, and M. Elad, "Convolutional neural networks analyzed via convolutional sparse coding," *J. Mach. Learn. Res.*, vol. 18, pp. 1–52, 2017.
- [29] V. Papyan, Y. Romano, J. Sulam, and M. Elad, "Theoretical foundations of deep learning via sparse representations: A multilayer sparse model and its connection to convolutional neural networks," *IEEE Signal Process. Mag.*, vol. 35, no. 4, pp. 72–89, 2018, doi: 10.1109/MSP.2018.2820224.
- [30] S. S. Chen, D. L. Donoho, and M. A. Saunders, "Atomic decomposition by basis pursuit," *SIAM Rev.*, vol. 43, no. 1, pp. 129–159, 2001.
- [31] M. Elad, *Sparse and redundant representations: From theory to applications in signal and image processing*. Springer New York, 2010.
- [32] J. Sulam, A. Aberdam, A. Beck, and M. Elad, "On multi-layer basis pursuit, efficient algorithms and convolutional neural networks,"

- IEEE Trans. Pattern Anal. Mach. Intell.*, vol. 42, no. 8, pp. 1968–1980, 2019.
- [33] S. Ioffe and C. Szegedy, “Batch normalization: Accelerating deep network training by reducing internal covariate shift,” in *International conference on machine learning*, 2015, pp. 448–456.
- [34] X. Glorot, A. Bordes, and Y. Bengio, “Deep sparse rectifier neural networks,” in *Proceedings of the fourteenth international conference on artificial intelligence and statistics*, 2011, pp. 315–323.
- [35] A. Paszke *et al.*, “PyTorch: An imperative style, high-performance deep learning library,” *arXiv*, no. NeurIPS, 2019.
- [36] G. J. Brostow, J. Shotton, J. Fauqueur, and R. Cipolla, “Segmentation and recognition using structure from motion point clouds,” *Lect. Notes Comput. Sci. (including Subser. Lect. Notes Artif. Intell. Lect. Notes Bioinformatics)*, vol. 5302 LNCS, no. PART 1, pp. 44–57, 2008, doi: 10.1007/978-3-540-88682-2\_5.
- [37] Y. Liu, J. Yao, X. Lu, R. Xie, and L. Li, “DeepCrack: A deep hierarchical feature learning architecture for crack segmentation,” *Neurocomputing*, vol. 338, pp. 139–153, 2019, doi: 10.1016/j.neucom.2019.01.036.
- [38] D. P. Kingma and J. Ba, “Adam: A method for stochastic optimization,” *arXiv Prepr. arXiv1412.6980*, 2014.
- [39] I. J. Goodfellow *et al.*, “Generative adversarial networks,” *arXiv Prepr. arXiv1406.2661*, 2014.
- [40] R. Sequiera *et al.*, “Exploring the effectiveness of convolutional neural networks for answer selection in end-to-end question answering,” *arXiv Prepr. arXiv1707.07804*, 2017.